Simple energy-budget model for yolk-feeding stages of Atlantic cod (*Gadus morhua*)

Tjalling Jager[a,], Raymond Nepstad[b], Bjørn Henrik Hansen[b], Julia Farkas[b]

[a] *DEBtox Research, De Bilt, the Netherlands*
[b] *SINTEF Ocean, Environment and New Resources, Trondheim, Norway*

Abstract

Atlantic cod (*Gadus morhua*) is a commercially important species, and therefore, understanding the influence of environmental factors and anthropogenic stressors on its early life stages is of considerable relevance. In this contribution, we apply a simple and generic energy-budget framework (DEBkiss) to data for the yolk-feeding stages of cod. The model is capable of explaining the changes in yolk volume, dry weight, oxygen use and body length, simultaneously with a small number of parameters. The calibrated model was subsequently successfully tested with other data sets. Interestingly, the light conditions after hatching affect growth and respiration rates, which is traced to a change in the maintenance costs (linked to swimming activity). Despite the satisfactory performance of the model, several uncertainties remain. Especially the bioenergetics around the point of complete yolk absorption require further attention, which is complicated by the fact that the behaviour around this point differed between data sets. The presented model can be used for exploring effects of stressors on early-life stages of cod, and

Email address: tjalling@debtox.nl (Tjalling Jager)
URL: http://www.debtox.nl/ (Tjalling Jager)

likely for other aquatic egg-laying species as well.

Keywords: energy budget, DEBkiss, *Gadus morhua*, embryonic development, modelling, yolk absorption

1. Introduction

Atlantic cod (*Gadus morhua*) is a fish species of substantial economic importance, and therefore there is considerable interest in the effects of environmental factors and stressors (such as temperature and xenobiotics) on its life history. The early-life stages of fish are crucial for recruitment of both natural and cultured fish stocks (Kamler, 2008), and are regularly specifically sensitive to chemical stress (see e.g., Petersen and Kristensen, 1998; Massei et al., 2015). Interpreting, understanding and ultimately predicting stressor effects on the life history requires bioenergetic models (Jager et al., 2013). In all animals, food is used to fuel the energy-demanding processes of maintenance, activity, growth, development and reproduction. In doing so, the individual needs to obey the conservation laws for mass and energy, which helps to structure the modelling efforts.

The yolk-feeding stages are of particular interest from a bioenergetic viewpoint as most of them can be considered as semi-closed systems (Heming and Buddington, 1988): practically all of the energy that the developing embryo uses for its development is locked inside the egg in the form of endogenous yolk. This makes them ideal objects to study the effects of environmental factors and stresses on their energy budget. Specific bioenergetic models have been proposed for fish development over the yolk-feeding stages (Beer and Anderson, 1997; Jaworski and Kamler, 2002), but we aim for a more

general treatment, embedding the yolk stages into the rest of the life cycle and linking fish to other animal species. Dynamic Energy Budget (DEB) theory (Jusup et al., 2017; Sousa et al., 2010) offers such a generic and inclusive bioenergetics representation, covering the entire life cycle (from egg to death) for all forms of life. The DEBkiss framework (Jager et al., 2013; Jager, 2016) is derived from DEB theory by applying several simplifications to ease parameterisation, interpretation and practical applications, such as in interpreting the effects of chemical stress (Barsi et al., 2014) and ocean acidification (Jager et al., 2016).

The most prominent simplification in DEBkiss is the removal of 'reserve' as a state variable in the model. For many applications, this turns out to be an acceptable simplification (see list of papers at `http://www.debtox.info/debkiss_appl.html`). The result is a simple model for bioenergetics of (ectothermic) animals over their entire life cycle, including the embryonic stages (Jager et al., 2013; Barsi et al., 2014). However, for eggs, the removal of reserve required some additional thought. DEB theory considers the yolk as part of the reserve, and clearly, no model for embryo bioenergetics can work without a state variable that considers yolk. In DEBkiss, yolk is treated as a buffer, handed over by the mother to the egg, which is assimilated, in a similar fashion as assimilation of food by the free-swimming feeding stages. This assumption is quite similar to the assumptions made for yolk absorption by Beer and Anderson (1997) and Jaworski and Kamler (2002).

To test the performance of the simple DEBkiss model for egg development and yolk feeding, we apply it to data for the Atlantic cod. Once parameterised and tested, this model may prove to be useful to interpret and predict the

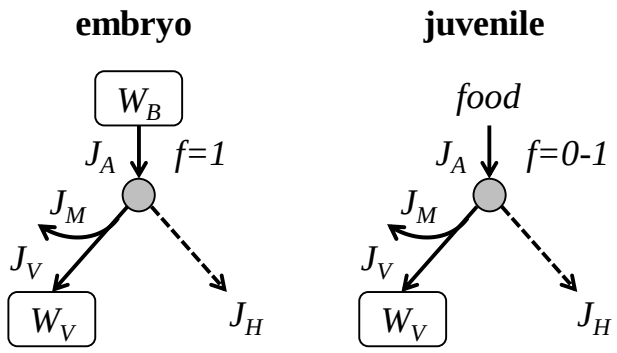

Figure 1: Schematic representation of the DEBkiss model for embryos and juveniles; in a DEB context, the transition from embryo to juvenile is defined by the start of (the ability for) external feeding. State variables are egg buffer or yolk (W_B) and structure (W_V), and fluxes are for assimilation (J_A), maintenance (J_M), growth (J_V) and maturation (J_H). The scaled functional response f is 1 for embryos (*ad libitum*) and depends on food availability for juveniles (zero when no food is present). Grey circle is a split of the assimilation flux, with a fraction of κ allocated to maintenance and growth.

effects of environmental changes and stressor effects on the yolk-feeding stages of cod. As the DEBkiss model is generic, it can then likely be applied to other fish species (and even other egg-laying animals) as well.

2. Methods

2.1. Basic model for embryos

A detailed description of DEBkiss can be found elsewhere (Jager et al., 2013; Jager, 2016); below a summary is given as far as relevant for the early life stages (reproduction is excluded from the model description here). The model structure for these stages is schematically shown in Figure 1, and all symbols used in this study are summarised in Table 1. Note that in DEB terminology, the embryo is the initial stage of the life cycle where the animal

does not feed exogeneously, and the juvenile stage starts with the ability to feed exogeneously. The points of hatching and metamorphosis (the end of the larval stage) are not stage switches from an energetic viewpoint.

Over its early development, the embryo goes through a series of events, for cod described in detail by Hall et al. (2004). These events represent major changes in morphology of the embryo, but for our DEBkiss model, all this detail will be ignored. The egg is treated as consisting of two state variables: the mass of the egg buffer W_B (representing the yolk) and the mass of structure W_V (representing the embryo or larvae without the yolk sac). The egg buffer is assimilated at a rate J_A, and structural mass increases with a growth flux J_V:

$$\frac{d}{dt}W_B = -J_A \quad \text{until } W_B = 0, \text{ with } W_B(0) = W_{B0} \tag{1}$$

$$\frac{d}{dt}W_V = J_V \quad \text{with } W_V(0) = W_{V0} \tag{2}$$

To facilitate the links between mass, surface area, and body length, it is practical to work with volumetric length (L), which is the cubic root of structural volume (using the dry-weight density d_V). Volumetric length can in turn be linked to more practical length measures (L_w, e.g., standard length, SL, in fish) by a shape-correction coefficient (δ_M):

$$L^3 = \frac{W_V}{d_V} \quad \text{and } L_w = \frac{L}{\delta_M} \tag{3}$$

Reported water content for cod larvae (4.5-10 mm SL) is around 85% (Finn et al., 2002). This implies that we can use $d_V = 0.15$ mg/mm^3 as a reasonable estimate for the density of structure. In our calibration data set (Finn et al.,

1995), yolk is expressed as a volume, and hence we also need a dry-weight density for the egg buffer (d_B). We leave this as a free parameter to be estimated in the fit to the data, as we have no direct information on the yolk properties. Measurements on total fresh eggs (Finn et al., 1995) suggest a value close to 0.07 mg/mm^3.

Next, we need to fill in the mass fluxes for the various processes. The assimilation flux (J_A) is proportional to a surface area of the animal, and the maintenance flux (J_M) to a volume. A fraction κ of the assimilation flux is used (with a certain efficiency, y_{VA}) for growth (J_V); the remainder (here denoted as J_H) is assumed to be dissipated. In the DEB context, the flux J_H is used for maturity and maturity maintenance; even though these processes are not explicitly followed here, specification of this flux is needed to close the mass balance and for the calculation of respiration rates later on. The mass fluxes are defined as follows:

$$J_A = f J^a_{Am} L^2 \quad (\text{if } W_B > 0 \text{ then } f = 1) \tag{4}$$

$$J_M = J^v_M L^3 \tag{5}$$

$$J_V = y_{VA}(\kappa J_A - J_M) \tag{6}$$

$$J_H = (1 - \kappa) J_A \tag{7}$$

The scaled functional response f is included in the assimilation flux J_A, and is a function of food availability (1 represents *ad libitum* conditions and 0 complete starvation). For yolk-feeding stages, we assume $f = 1$ until yolk runs out. However, what happens when the larva starts to feed exogeneously? The larvae obtain the ability to feed after development of a functional jaw

and hindgut (Hall et al., 2004), which is generally before the yolk is fully exhausted (Kamler, 2008; Heming and Buddington, 1988). This implies that we, at some point, need to consider two food sources. We leave the question of mixed feeding open at the moment, as the experimental data sets that we use did not offer any food to the animals. The resulting instantaneous switch from $f = 1$ to $f = 0$ is unrealistic in detail; in practice, we will likely see a smoother transition from yolk-feeding to starvation.

2.2. Response to starvation and temperature

When the allocated assimilation flux κJ_A is insufficient to cover the maintenance costs J_M, the animal needs to deviate from the rules provided above. Jager et al. (2013) proposed a simple model to deal with this problem in two stages (see supporting information). Here, we can simplify the model to a single stage as we assumed an instantaneous switch from $f = 1$ to $f = 0$ when yolk runs out. In the absence of yolk or external food, the animal will shrink, i.e., use structural tissue to pay the maintenance cost:

$$J_V = -J_M / y_{AV} \text{ and } J_H = 0 \tag{8}$$

Shrinking (negative value for J_V) implies that W_V will decrease, but not necessarily L_w. If we use standard length as our size measure, it will be determined by the length of the notochord, which is unlikely capable of shrinking.

Temperature is clearly an important factor for the bioenergetics, and increasing the temperature speeds up development (Geffen et al., 2006). In DEB applications, it is generally assumed that all rate constants (with a dimension that includes 'per time') scale in the same way with temperature.

We can use the Arrhenius relationship to scale from a reference temperature T^* to the actual temperature T (both in Kelvin). All rate constants have to be multiplied by:

$$F_T = \exp\left(\frac{T_A}{T^*} - \frac{T_A}{T}\right) \tag{9}$$

where T_A is the Arrhenius temperature in Kelvin. Lika et al. (2011) suggest a value of 8000 K as typical value.

2.3. Link between mass fluxes and oxygen use

Measurements of oxygen use provide valuable insights into the bioenergetics of the yolk-feeding stages. They are easier to interpret than measurements on the externally-feeding stages: the embryos continue all of the regular metabolic work during the measurement of oxygen use, as they have a constant supply of energy. In contrast, feeding stages will usually be fasted for some time before measurement, with unclear consequences for the bioenergetics (see Jager and Ravagnan, 2016). Oxygen use is related to the mass fluxes that dissipate. The total dissipation flux (J_D), as relevant in the context of the early life stages, is given by:

$$J_D = J_M + J_H + J_{Vo} \tag{10}$$

Where J_{Vo} indicates the overhead costs for growth or shrinking:

$$J_{Vo} = \begin{cases} J_V(1 - y_{VA})/y_{VA} & \text{if } J_V \geq 0 \\ J_V(y_{AV} - 1) & \text{if } J_V < 0 \end{cases} \tag{11}$$

The dissipation flux is a mass flux (in mg of assimilates per day). In practice, respiration is often expressed in terms of oxygen use. To convert this mass

flux to moles of oxygen, we need the carbon content of biomass or yolk for the species (d_C; we take 0.4 mg/mg as a representative value), the molar mass of carbon (12 g/mol), and the respiratory quotient (F_{RQ}). This quotient is the moles of CO_2 (and thus also the moles of C) eliminated per mole of O_2 taken up (we take 0.8 as a reasonable value). For our validation study, we need to convert moles of oxygen further to microliters, which requires the molar mass of oxygen (32 g/mol) and its density (1.43 g/L at 0°C).

2.4. Implementation and calibration

The model was implemented in Matlab using the generic BYOM platform (http://www.debtox.info/byom.html). Optimisation was performed by maximising an overall likelihood function (assuming normally-distributed and independent errors). Confidence intervals were calculated by profiling the likelihood. All data were extracted from the original publications using the freeware PlotReader (http://jornbr.home.xs4all.nl/plotreader). The data are used in the form, and with the units, as given in the original publications; the model outputs (W_B, W_V and J_D) were recalculated to match the type and unit of the data set. This is done to keep the data points unaffected by the uncertainty in the transformations. The only recalculation is the derivation of yolk dry weight in the data sets of Solberg and Tilseth (1984,?). This is calculated from the total weights for eggs/larvae and chorion weight (and thus requires no uncertain transformations).

We selected the data set from Finn et al. (1995) to calibrate the model, as it contains measurements on different endpoints from the same group of animals: yolk volume, dry weights, standard length (after hatch), and respiration rate. The experiments were perfomed at 6°C, with the eggs initially

kept under continuous light, but switching to a 14:10 light-dark regime post hatching. The measured dry weight of the complete egg requires some further thought as this measurement includes contributions from the yolk, the structural part of the embryo, and the chorion of the egg. For the chorion, we take a fixed value of 0.020 mg, based on the measurements of Solberg and Tilseth (1984).

For the respiration data, two series of measurements were presented: one in light and one in dark conditions. For the egg stage and several days after hatching, these measurements were very similar, but around the time that yolk ran out, a profound difference was observed. A square-root transformation was applied for this data set to increase the importance of the initial respiration measurements of the early egg stages, and decrease the importance of the post-hatching measurements (which is useful in view of the variation induced by light conditions).

2.5. Model testing

To test the model and its parameterisation, a second (independent) data set (Solberg and Tilseth, 1984) was used as model corroboration. These authors report measurements of dry weights of chorion, total egg, whole larvae (incl. yolk), larvae with dissected yolk, as well as standard length post hatch. These experiments were performed at 5°C under a 12:12 hour light regime, and used two batches of eggs from different females. Since these experiments were done at a slightly different temperature (5°C instead of 6°C), we calculated a temperature correction factor (Eq. 9), which is applied to both rate constants (specific assimilation and specific maintenance rates).

The initial amount of yolk (W_{B0}) was calculated from the mean weight of

the total fresh egg in this study (0.107 mg) minus the chorion and the value of W_{V0} (Table 1). Additionally, the same study reports some respiration data, post-hatching, from other batches of eggs. We added the respiration data from Serigstad and Adoff (1985), which covers the egg stage as well (also performed at 5°C). For all respiration data sets, we do not have the corresponding development of larval and yolk mass for the same batches of eggs, which implies additional uncertainty.

2.6. Effects of light and temperature

Solberg and Tilseth (1984, 1987) also report an experiment with hatched larvae, reared under different temperatures (3, 5 and 7°C) and light conditions (constant darkness or constant light). Total dry weight, dry weight of larvae with dissected yolk, and standard length were reported. Initial amounts of yolk and structure were fixed to the first measurements (shortly after hatching). These data only have information for the end of the yolk-feeding stage and the subsequent starvation phase. We fitted both the specific assimilation rate and the specific maintenance rate on each treatment (κ was fixed to the value established in the calibration, see Table 1), and only show the parameter estimates (fits are provided in supporting information).

3. Results and discussion

3.1. Model calibration

The model fit to the calibration data (Finn et al., 1995) is shown in Figure 2. The four data sets are fitted simultaneously with only seven parameters; an average of less than two parameters per data set (parameter estimates

Sym.	Explanation	Value (C.I.)	Unit
	Primary parameters		
f	Scaled functional response	1/0 (n.e.)	–
J^a_{Am}	Maximum area-specific assimilation rate	16.0 (14.7-17.1) 10^{-3}	mg mm^{-2} d^{-1}
J^v_M	Volume-specific maintenance costs	4.37 (3.87-5.02) 10^{-3}	mg mm^{-3} d^{-1}
y_{AV}	Yield assimilates on structure (shrinking)	0.8 (n.e.)	mg mg^{-1}
y_{VA}	Yield structure on assimilates (growth)	0.8 (n.e.)	mg mg^{-1}
κ	Fraction of assimilation flux for soma	1 (0.949-1)	–
	Initial states		
W_{B0}	Assimilates in freshly-laid egg	100 (96.9-104) 10^{-3}	mg
W_{V0}	Structure in freshly-laid egg	2.35 (1.48-3.64) 10^{-3}	mg
	Conversions		
d_B	Dry-weight density of egg buffer	0.0745 (0.0714-0.0796)	mg mm^{-3}
d_C	Carbon content of yolk and structure	0.40 (n.e.)	mg mg^{-1}
d_V	Dry-weight density of structure	0.15 (n.e.)	mg mm^{-3}
F_{RQ}	Respiratory quotient	0.8 (n.e.)	–
W_c	Weight of chorion of egg	0.020 (n.e.)	mg
δ_M	Shape correction coefficient	0.157 (0.151-0.162)	–
	Fluxes and state variables		
J_A	Mass flux for assimilation		mg d^{-1}
J_D	Total mass flux that is dissipated		mg d^{-1}
J_H	Mass flux for maturation/maturity maint.		mg d^{-1}
J_M	Mass flux for maintenance		mg d^{-1}
J_V	Mass flux for structure (growth/shrinking)		mg d^{-1}
J_{Vo}	Overhead costs for growth/shrinking		mg d^{-1}
W_B	Mass of assimilates buffer in egg		mg
W_V	Mass of structural body		mg
	Derived or intermediate variables		
L	Volumetric body length		mm
L_w	Physical body length (e.g., SL)		mm

Table 1: Explanation of symbols used in this study. For parameters and constants, values are given, which are either fitted (see Fig. 12; , 95% confidence interval in parentheses) or fixed (n.e., not estimated). Values for the yield coefficients are taken from Jager et al. (2013); other fixed values explained in the text. When yolk is present $f = 1$, and otherwise $f = 0$. Rate constants represent a temperature of 6°C.

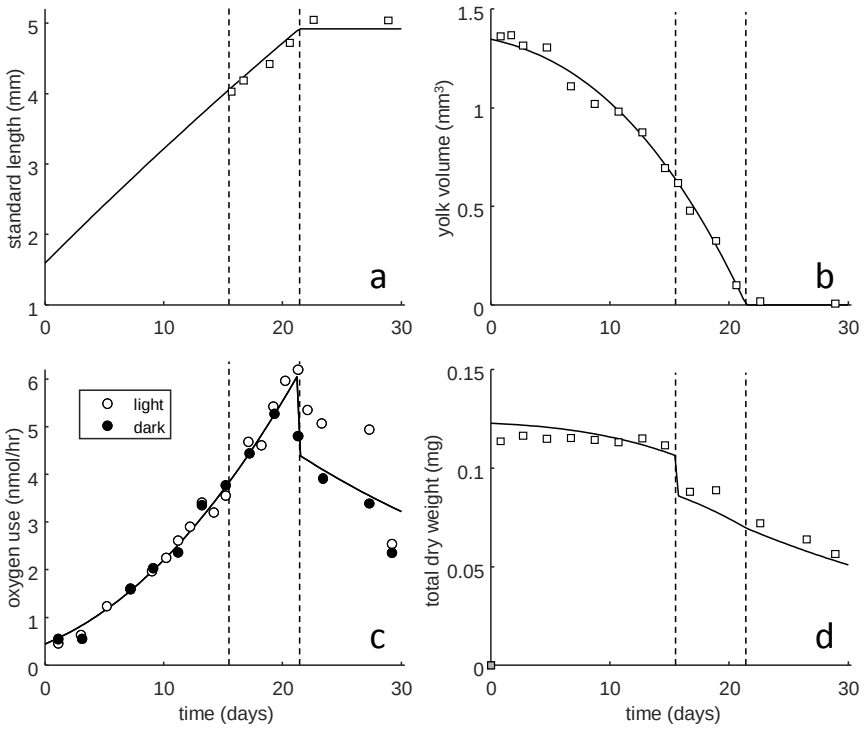

Figure 2: Fit of the DEBkiss model on data from Finn et al. (1995) at 6°C. For the respiration plot (panel c), different symbols are used for measurements under light or dark conditions. The first broken line indicates the approximate time for hatching in the experiment, and the second broken line represents the modelled time for total yolk absorption. The jump in dry weight is the loss of the chorion at hatching (chorion weight taken as 0.020 mg).

with confidence intervals are given in Table 1). The model itself has only three parameters that need to be fitted. Additionally, there are two initial states (initial mass of structure and yolk) that need to be estimated, as well as two conversion factors to link state variables (mass) to observations (yolk volume and standard length). Note that the estimate for the density of yolk is very close to the value estimated from the total fresh egg (0.07 mg/mm^3; Finn et al., 1995).

Overall, the fit is very good, but several issues can be observed on closer inspection. Starting with the total dry weight (Fig. 2d): the model predicts a decrease of total dry weight over the egg stage, which is not shown in the data. As the egg membrane severely restricts uptake of solutes, the burning of yolk (mass flux J_D) should lead to a loss of dry weight as the embryo develops (closely linked to the observed respiration rate). Eggs may be taking up some minerals from water, but no increase in ash content was observed in this study (Finn et al., 1995). Further, eggs and larvae appear to be capable of absorbing dissolved organic molecules from water, although the contribution to the mass and energy budget is expected to be negligible (Heming and Buddington, 1988). A decrease in total egg weight was observed in the validation data set (Solberg and Tilseth, 1984), so the lack of a decrease here could represent a measurement bias.

The respiration rate (Fig. 2c) is nicely fitted up to the point where the yolk runs out. At that point, there is also a clear difference between the respiration rate measured in light and in dark conditions. The model predicts a sharp drop in respiration rate when yolk runs out, as the scaled functional response switches instantly from $f = 1$ to $f = 0$. As a result of this transition

to complete starvation, growth switches to shrinking to match the maintenance needs, which leads to a lower total dissipation flux. As starvation progresses, respiration decreases as also the total amount of structure to be maintained decreases. This pattern is, in general, consistent with the data, although there is a considerable difference between the respiration data in light and dark conditions. The animals in the light clearly have a higher respiration rate after complete yolk absorption than predicted, which can be linked to an increased swimming activity (see Solberg and Tilseth, 1984). The role of swimming activity in the energy budget is discussed further in Section 3.3.

The increase in standard length over time (Fig. 2a) is well matched by the model (note that animals cannot shrink in length, even though they do shrink in dry weight). However, growth seems to increase for slightly longer than predicted. This might be caused by experimental difficulties of accurately measuring yolk volume close to the point of complete resorption. It is also possible that some resources have already been irreversibly allocated to length increase (notochord growth).

The estimate for κ is very high; virtually all of the assimilated energy from yolk is used for maintenance and growth. This value is linked to the fixed value for the growth efficiency (y_{VA}), and to the estimated specific maintenance rate (J_M^v), which in turn relies on the assumption that the shrinking of the larvae is linked to the maintenance requirements only. Given that the specific assimilation rate is severely restricted by the observed yolk absorption, these three parameters (κ, y_{VA} and J_M^v) determine the three fluxes contributing to dissipation (see Eq. 10), and hence the efficiency with

which yolk is turned into structural biomass. For example, assuming a higher growth efficiency ($y_{VA} = 0.90$) allows κ to decrease ($\kappa = 0.93$), with very little effect on the goodness-of-fit. It will be difficult in practice to determine the value of the yield coefficients, although this is unlikely to affect practical applications of the model.

The estimated value for the specific maintenance rate is very similar to the values established for two krill species (Jager and Ravagnan, 2016), when using the same reference temperature (assuming an Arrhenius temperature of 8000 K). The specific assimilation rate is, however, lower, which is surprising as cod will obviously grow to much larger sizes than krill (maximum volumetric length is determined by $\kappa J^a_{Am}/J^v_M$). The solution to this conundrum lies in the fact that fish accelerate metabolically after the start of feeding (Kooijman et al., 2011), which involves an increase of the specific assimilation rate for some time after yolk has disappeared. This allows these species to reach much larger sizes than indicated by their embryonic stage, and also explains the deviation from von Bertalanffy growth when early stages are included in the growth curve. Such an acceleration of growth (relative to von Bertalanffy growth) was observed for larval cod by Otterlei et al. (1999) as a clear up-curving for the length-age relationship.

3.2. Model testing

Next, the parameterised model is tested with data from Solberg and Tilseth (1984). The correspondence between model and data is quite convincing (Fig. 3), especially given the fact that no parameters are fitted. Interestingly, development in this study (and for the additional respiration data from Serigstad and Adoff, 1985, in panel c) was somewhat slower than

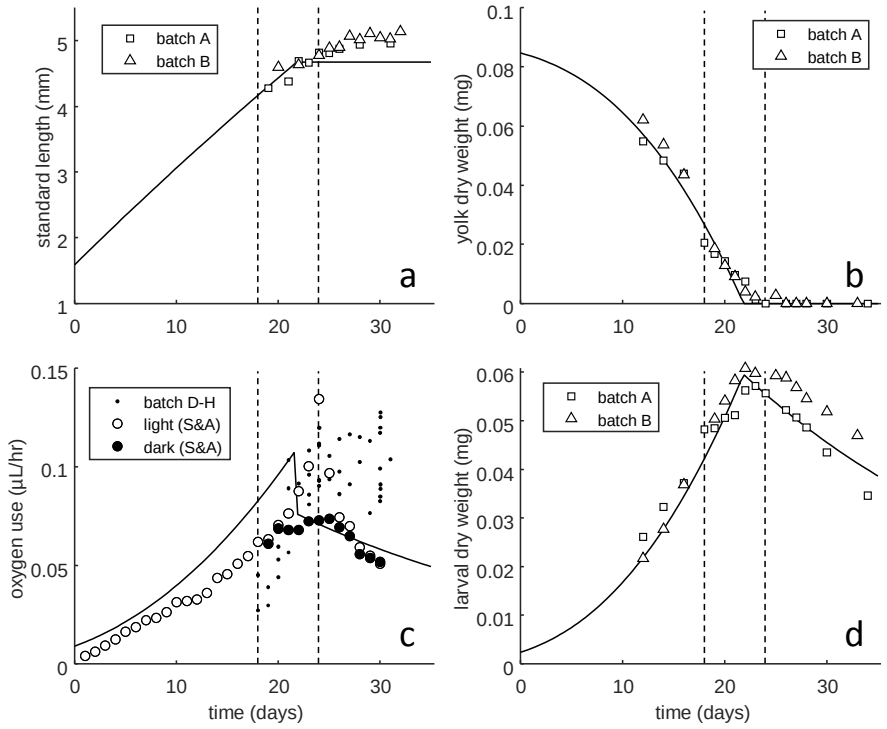

Figure 3: Predictions for additional data (Solberg and Tilseth, 1984) with different batches of eggs at 5°C. The respiration data light/dark (panel c) are taken from Serigstad and Adoff (1985). The model parameters were fixed to the best-fitting values from Table 1, with a temperature correction using Eq. 9. The broken lines indicate the approximate times for hatching and total yolk absorption, as observed in these experiments.

in the calibration study (Fig. 2). Hatching took place around day 18 (compared to day 16 in the calibration study), and complete yolk absorption after 24 days, or even later (compared to 21 days in the calibration). Furthermore, the final stage of yolk resorption seems to be somewhat slower than predicted from the model (Fig. 3b). It appears that the transition from *ad libitum* yolk feeding to complete starvation is more gentle than assumed in the model. Also, growth in length (Fig. 3a) continues for quite a while longer than predicted. These deviations from the model predictions were not observed to the same extent in the calibration data set (Fig. 2). It is tempting to include smoothing mechanisms, such as the internal reserve compartment of the standard DEB model (Sousa et al., 2010) or a limitation of the assimilation flux by the surface area of the yolk sac (see Beer and Anderson, 1997, and supporting information). However, such mechanisms are inconsistent with the rather rapid transition in respiration rate when yolk disappears (Fig. 2c), and were also not as clear in other batches of eggs from Solberg and Tilseth (1984) (see supporting information). More detailed data on growth and respiration would be needed to settle this question.

The respiration data from different batches of eggs (batch D-H in Fig. 3c) are not well matched by the model prediction. Before final yolk absorption the data are overestimated and afterwards underestimated. The reasons for this discrepancy are unclear. The data set from Serigstad and Adoff (1985) (with larvae reared under continuous light or darkness) shows a pattern that better matches the model predictions, although the data are shifted to the right, as already mentioned. Interestingly, the respiration data for constant light show a closer resemblance to the pattern predicted by the model; hence,

the model suggests that respiration rates are depressed in darkness, rather than being stimulated by light. Respiration rates are, however, difficult to interpret without measurements for yolk and structural mass on the same animals.

We can now also use the model to predict embryonic development under other conditions. For example, we can predict how the duration of yolk feeding will change with egg size. Model simulation shows that yolk feeding will be extended by a factor of 1.4 longer for a doubling of the yolk content, which is well in line with the factor of 1.3 mentioned by Heming and Buddington (1988) for cod and herring.

3.3. Effect of temperature and light

The last data sets we used are also from Solberg and Tilseth (1984, 1987), but consider only the changes in yolk weight, larval weight, and SL, post hatching (in absence of food). These experiments were performed at three temperatures and at constant light or constant darkness. All six data sets were fitted, and the fitted parameters are plotted in Figure 4 (individual fits shown in supporting information). The values for the specific maintenance rate are well in line with the value determined earlier for 6°C (Table 1); the calibrated value is in between the estimates for total light and total darkness. However, the specific assimilation rates are roughly half of what was estimated from the calibration data. This is likely linked to a slower use of the final portion of the yolk, as discussed above (these six data sets only follow the larvae when the yolk is already almost exhausted).

Specific assimilation rates are somewhat lower in the light, but the confidence intervals mostly overlap. However, for the specific maintenance rate,

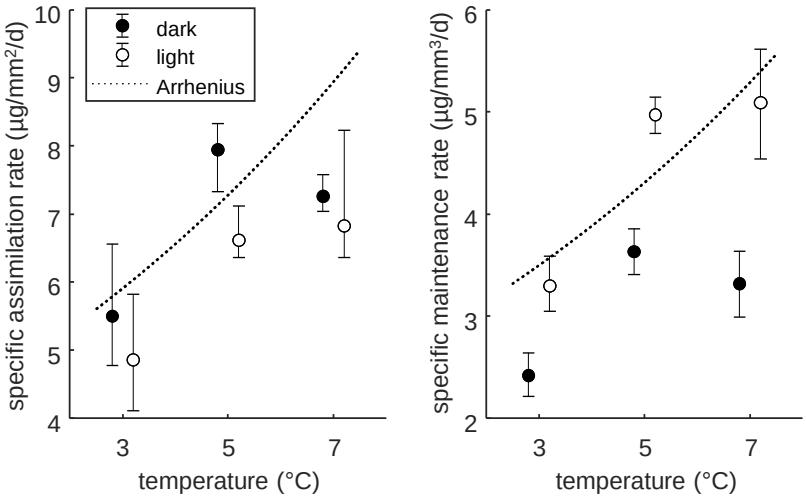

Figure 4: Parameter values with 95% confidence interval from fits on data for post-hatching development without food, at three temperatures and continuous light or darkness (Solberg and Tilseth, 1984, 1987). Points are slightly shifted horizontally to enhance readability. An Arrhenius relationship with an Arrhenius temperature of 8000 K is shown for reference. The κ was fixed to the value in Table 1.

there is a clearly elevated rate constant (on average 42% across the tested temperatures) in the light at all temperatures. As shown in Figure 2c and 3c, animals kept in the light also showed higher respiration rates, which is likely linked to their higher swimming activity (Solberg and Tilseth, 1984). Thus, we can infer that swimming activity shows up in the energy budget as a component of the maintenance rate. Since maintenance costs compete with growth, and cause shrinking when the yolk has run out, they show up in the pattern of structural body mass over time. In DEB models, the maintenance rate is generally taken as a constant, lumping the energy requirements for tissue maintenance and activity (Sousa et al., 2010). This assumption may need some more detailed consideration, especially for fish larvae experiencing a diurnal cycle.

Figure 4 also shows an Arrhenius relationship, going through the mean value of each rate constant at 5°C. The increase in the rate constants from 3-5°C is consistent with this prediction, but there is no further increase to be observed from 5-7°C. The reason for this lack of temperature effect is unclear, but may relate to experimental problems. Interestingly, the data on hatching time, provided in the same paper, do show a smoothly decreasing relationship with temperature, as do the data sets provided in Geffen et al. (2006) over a much wider temperature range.

4. Conclusions

We applied the generic energy-budget model DEBkiss to extensive data for early life stages of cod. In general, this simple model provided an excellent explanation of the data sets. Some aspects in some of the data indicate

the presence of a smoothing mechanism (delayed response of length growth to yolk depletion, and decreased absorption rates when the yolk sac is very small), but the rather rapid response of the respiration rate on yolk exhaustion argues against it. Clearly, all models are wrong in detail, and simple models, like energy-budget approaches, obviously lack many of the morphological (e.g., Hall et al., 2004) and biochemical (e.g., Finn et al., 1995) details. In the end, the utility of these models must be judged in light of the specific application for which they are used. The applications that we envisage for this model are in the interpretation and prediction of the effects of (combinations of) environmental factors and stressors on embryonic development.

The type of application that we specifically see is in the interpretation of toxicity tests with embryos. This is particularly pertinent as toxicity tests with embryonic fish are increasingly being used as alternatives for testing with subsequent (and legally-protected) life stages (e.g., Embry et al., 2010). Even though more-detailed evaluation will be needed, work on the effects of acetone on pond-snail eggs (Barsi et al., 2014) already provided substantial support. To apply the model to toxicants, it needs to be extended with a toxicokinetics module (see Jager, 2016). For eggs and yolk-feeding larval stages, additional consideration will be necessary. For example, the rate of chemical exchange for the egg stage is considerably slower than for the larvae post hatching (Petersen and Kristensen, 1998). Furthermore, there may also be stage-specific mechanisms of toxicity in the early life stages (see e.g., Massei et al., 2015). It should furthermore be noted that energy-budget models are of little help in the interpretation of non-energy related endpoints such as malformations. Nevertheless, such endpoints will still require knowledge on

toxicokinetics, and it is likely that toxicokinetics is affected by the patterns of structural and yolk mass over time.

In this study, we only considered the yolk-feeding stages. However, it is good to realise that DEBkiss is a model for the full life cycle of animals. Full-life cycle bioenergetic models have a range of potential applications, for example in conjunction with individual-based population models (IBMs) to assess population development under time-varying environmental conditions. Models based on DEBkiss have been linked to IBMs in some cases, such as for salmon (Fiechter et al., 2015) and krill Groeneveld et al. (2015). Even though more work is needed to test the embryo-specific part of the model in detail, the advantage of DEB-based approaches is that the embryonic stage is treated in a manner that is consistent with the rest of the life cycle, and consistent with other forms of life. The only cod-specific aspect of the model are the parameter values. This generic approach to bioenergetics will generally be a more efficient strategy in understanding and interpreting stressor effects than developing a new model for each life stage and each species.

5. Acknowledgements

This work was conducted as part of the DiTail project, financed by the Research Council of Norway (grant no. 281093).

References

Barsi, A., Jager, T., Collinet, M., Lagadic, L., Ducrot, V., 2014. Considerations for test design to accommodate energy-budget models in ecotox-

405 icology: a case study for acetone in the pond snail *Lymnaea stagnalis*.
406 Environmental Toxicology and Chemistry 33 (7), 1466–1475.

407 Beer, W. N., Anderson, J. J., 1997. Modelling the growth of salmonid em-
408 bryos. Journal of Theoretical Biology 189 (3), 297–306.

409 Embry, M. R., Belanger, S. E., Braunbeck, T. A., Galay-Burgos, M., Halder,
410 M., Hinton, D. E., Léonard, M. A., Lillicrap, A., Norberg-King, T., Whale,
411 G., 2010. The fish embryo toxicity test as an animal alternative method
412 in hazard and risk assessment and scientific research. Aquatic Toxicology
413 97 (2), 79–87.

414 Fiechter, J., Huff, D. D., Martin, B. T., Jackson, D. W., Edwards, C. A.,
415 Rose, K. A., Curchitser, E. N., Hedstrom, K. S., Lindley, S. T., Wells,
416 B. K., 2015. Environmental conditions impacting juvenile Chinook salmon
417 growth off central California: an ecosystem model analysis. Geophysical
418 Research Letters 42 (8), 2910–2917.

419 Finn, R. N., Fyhn, H. J., Evjen, M. S., 1995. Physiological energetics of
420 developing embryos and yolk-sac larvae of Atlantic cod (*Gadus morhua*)
421 .I. respiration and nitrogen metabolism. Marine Biology 124 (3), 355–369.

422 Finn, R. N., Rønnestad, I., van der Meeren, T., Fyhn, H. J., 2002. Fuel
423 and metabolic scaling during the early life stages of Atlantic cod *Gadus*
424 *morhua*. Marine Ecology Progress Series 243, 217–234.

425 Geffen, A. J., Fox, C. J., Nash, R. D. M., 2006. Temperature-dependent
426 development rates of cod *Gadus morhua* eggs. Journal of Fish Biology
427 69 (4), 1060–1080.

Groeneveld, J., Johst, K., Kawaguchi, S., Meyer, B., Teschke, M., Grimm, V., 2015. How biological clocks and changing environmental conditions determine local population growth and species distribution in antarctic krill (*Euphausia superba*): a conceptual model. Ecological Modelling 303, 78–86.

Hall, T. E., Smith, P., Johnston, I. A., 2004. Stages of embryonic development in the Atlantic cod *Gadus morhua*. Journal of Morphology 259 (3), 255–270.

Heming, T. A., Buddington, R. K., 1988. Yolk absorption in embryonic and larval fishes. In: Hoar, W. S., Randall, D. J. (Eds.), Fish Physiology. Vol. 11. Academic Press, pp. 407–446.

Jager, T., 2016. DEBkiss. A simple framework for animal energy budgets. Leanpub: https://leanpub.com/debkiss_book, Version 1.5.

Jager, T., Martin, B. T., Zimmer, E. I., 2013. DEBkiss or the quest for the simplest generic model of animal life history. Journal of Theoretical Biology 328, 9–18.

Jager, T., Ravagnan, E., 2016. Modelling growth of northern krill (*Meganyctiphanes norvegica*) using an energy-budget approach. Ecological Modelling 325, 28–34.

Jager, T., Ravagnan, E., Dupont, S., 2016. Near-future ocean acidification impacts maintenance costs in sea-urchin larvae: Identification of stress factors and tipping points using a DEB modelling approach. Journal of Experimental Marine Biology and Ecology 474, 11–17.

Jaworski, A., Kamler, E., 2002. Development of a bioenergetics model for fish embryos and larvae during the yolk feeding period. Journal of Fish Biology 60 (4), 785–809.

Jusup, M., Sousa, T., Domingos, T., Labinac, V., Marn, N., Wang, Z., Klanjscek, T., 2017. Physics of metabolic organization. Physics of Life Reviews 20, 1–39.

Kamler, E., 2008. Resource allocation in yolk-feeding fish. Reviews in Fish Biology and Fisheries 18 (2), 143–200.

Kooijman, S. A. L. M., Pecquerie, L., Augustine, S., Jusup, M., 2011. Scenarios for acceleration in fish development and the role of metamorphosis. Journal of Sea Research 66, 419–423.

Lika, K., Kearney, M. R., Freitas, V., Van der Veer, H. W., Van der Meer, J., Wijsman, J. W. M., Pecquerie, L., Kooijman, S. A. L. M., 2011. The "covariation method" for estimating the parameters of the standard Dynamic Energy Budget model I: philosophy and approach. Journal of Sea Research 66, 270–277.

Massei, R., Vogs, C., Renner, P., Altenburger, R., Scholz, S., 2015. Differential sensitivity in embryonic stages of the zebrafish (*Danio rerio*): The role of toxicokinetics for stage-specific susceptibility for azinphos-methyl lethal effects. Aquatic Toxicology 166, 36–41.

Otterlei, E., Nyhammer, G., Folkvord, A., Stefansson, S. O., 1999. Temperature- and size-dependent growth of larval and early juvenile Atlantic cod (*Gadus morhua*): a comparative study of Norwegian coastal

cod and northeast Arctic cod. Canadian Journal of Fisheries and Aquatic Sciences 56 (11), 2099–2111.

Petersen, G. I., Kristensen, P., 1998. Bioaccumulation of lipophilic substances in fish early life stages. Environmental Toxicology and Chemistry 17 (7), 1385–1395.

Serigstad, B., Adoff, G. R., 1985. Effects of oil exposure on oxygen consumption of cod eggs and larvae. Marine Environmental Research 17 (2-4), 266–268.

Solberg, T., Tilseth, S., 1984. Growth, energy consumption and prey density requirements in first feeding larvae of cod (*Gadus morhua* L.). In: Dahl, E., Danielsen, D. S., Moksness, E., Solemdal, P. (Eds.), The propagation of cod *Gadus morhua* L. Flødevigen rapportser 1. pp. 145–166.

Solberg, T. S., Tilseth, S., 1987. Variations in growth pattern among yolk-sac larvae of cod (*Gadus morhua* l.) due to differences in rearing temperature and light regime. Sarsia 72 (3-4), 347–349.

Sousa, T., Domingos, T., Poggiale, J. C., Kooijman, S. A. L. M., 2010. Dynamic energy budget theory restores coherence in biology. Philosophical Transactions of the Royal Society B-Biological Sciences 365 (1557), 3413–3428.